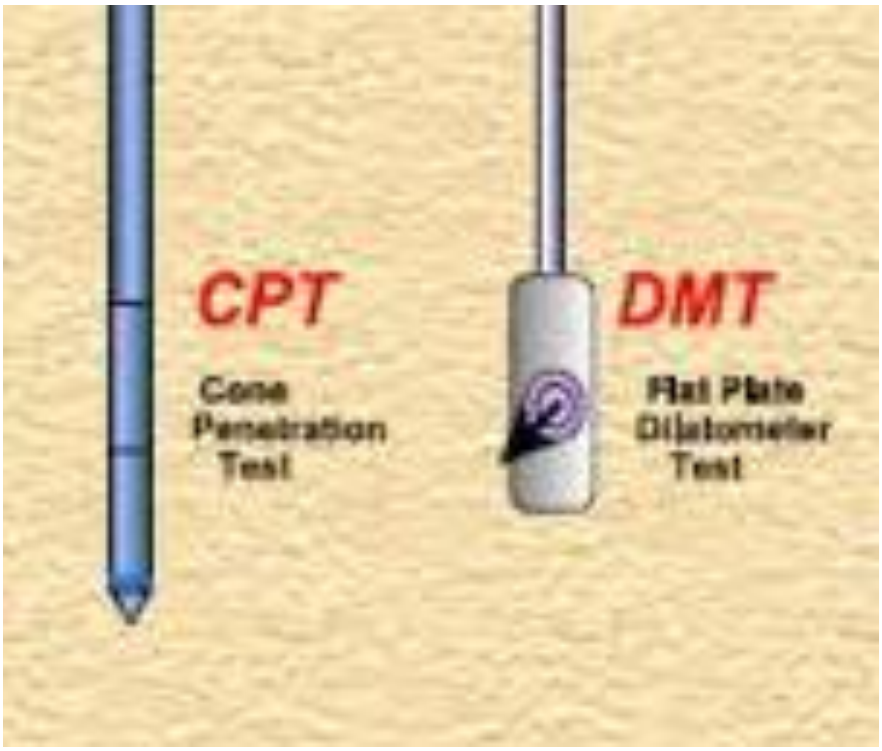

Massarsch, K.R. and Fellenius, B.H., 2019. Evaluation of vibratory compaction by in-situ tests. ASCE Journal of Geotechnical and Geoenvironmental Engineering, 145(12) 15 p. doi.10.1061/(ASCE)GT.1943-5606.0002166.

Case Study

Evaluation of Vibratory Compaction by In Situ Tests

K. Rainer Massarsch[1] and Bengt H. Fellenius, M.ASCE[2]

Abstract: The effect of vibratory compaction on a sandy deposit was investigated using different types of in situ methods. An important objective was to determine the change in soil resistance and horizontal stress at different time intervals after compaction. The horizontal stress, measured by different in situ methods, showed a significant and permanent increase due to vibratory compaction. The overconsolidation ratio of compacted sand was estimated based on the increase in horizontal stress using different methods. The tangent modulus method is shown to be a powerful concept for evaluating the settlement of compacted soil by considering the increase in soil stiffness (modulus number) and overconsolidation. The modulus number derived from in situ tests was compared with data reported in the literature. **DOI: 10.1061/(ASCE)GT.1943-5606.0002166.**

Author keywords: Cone penetration test; Dilatometer; Standard penetration test; Vibratory compaction; Horizontal stress; Overconsolidation ratio; Modulus.

Introduction

Although vibratory compaction is used extensively for solving different types of foundation and earthquake problems, the number of well-documented case histories is surprisingly small. On many of the projects reported in the geotechnical literature, details of soil conditions, prior to and at different time intervals after treatment, are often incomplete or rely only on one investigation method. In contrast, the following case history presents records of a project where different in situ methods were used to investigate the soil conditions before and at different time intervals after treatment. Detailed field investigations are reported and novel evaluation methods are used to answer the following questions: (1) How does the presence of intermediate fine-grained soil layers affect the results of vibratory compaction? (2) Do changes in soil strength and stiffness occur over time after treatment? (3) Can changes in horizontal stress due to vibratory compaction be measured? and (4) What are the consequences of such stress changes?

The change in horizontal stress caused by vibratory compaction is an important, but not generally appreciated, effect, yet it affects the performance of compacted sand when subjected to static or cyclic loading. Schmertmann (1985) pointed out that changes in horizontal effective stress caused by construction activities have a major impact on geotechnical design. Massarsch (1994) reported a case history of vibratory compaction of sand fill, where changes of horizontal stress were estimated from sleeve friction measurements using the cone penetration test (CPT). Howie et al. (2000) studied the effect of ground improvement by vibro-replacement. The compaction effect was measured by seismic cone penetration tests, full-displacement pressuremeter tests, and resistivity cone penetration tests. After ground treatment, changes were observed in cone stress, pore pressure response, shear wave velocity, and the characteristics of pressuremeter curves. The effect of vibratory compaction on soil stiffness and changes in horizontal stress determined from CPT was discussed by Massarsch and Fellenius (2002). A concept was described about how changes in horizontal stress can be included in a settlement analysis. The results of a comprehensive study by Asalemi (2006) confirm that significant changes in horizontal stress occur as a result of vibro-replacement. Also, Nguyen et al. (2014) showed that after vibratory ground treatment, the in situ horizontal effective stresses were significantly increased. Of particular interest in the context of this paper are the observed changes in horizontal stress as corroborated by the different methods. The authors highlight the importance of combining different types of tests to enhance understanding of changes in soil behavior achieved by ground treatment.

Annacis Island Vibratory Compaction

The case history presented in this paper describes the results of different in situ methods that can measure—directly or indirectly—increases in horizontal stress. The project site comprised a sandy soil deposit with interbedded layers of silt and clay, which was treated by resonance compaction to mitigate the liquefaction risk. In contrast to the case studies reported by Howie et al. (2000), Asalemi (2006), and Nguyen et al. (2014), ground treatment in the case reported here was carried out by vibratory compaction only, without the introduction of additional material. For details and additional information about the execution of the compaction work, reference is made to Neely and Leroy (1991) and Massarsch and Fellenius (2017). This paper focuses on the effects of vibratory compaction on the geotechnical properties of the soil at different time intervals after treatment and in particular on the change in horizontal stress following compaction.

The case history is exceptional in that several in situ testing methods were used in parallel to study the effect of vibratory compaction on a site susceptible to liquefaction. Although vibratory compaction was performed by one specific method (resonance compaction), the conclusions derived from the investigations are believed to be of general validity and applicable to other compaction methods. Extensive background material from a variety of soil investigation methods used at the project site and compiled

[1]Consulting Engineer, Geo Risk and Vibration Scandinavia AB, Ferievägen 25, Bromma, Stockholm SE 168 41, Sweden (corresponding author). ORCID: https://orcid.org/0000-0001-8906-7452. Email: rainer.massarsch@georisk.se

[2]Consulting Engineer, 2475 Rothesay Ave., Sidney, BC, Canada V8L 2B9. Email: bengt@Fellenius.net

Note. This manuscript was submitted on April 27, 2018; approved on June 28, 2019; published online on September 28, 2019. Discussion period open until February 28, 2020; separate discussions must be submitted for individual papers. This paper is part of the ***Journal of Geotechnical and Geoenvironmental Engineering***, © ASCE, ISSN 1090-0241.

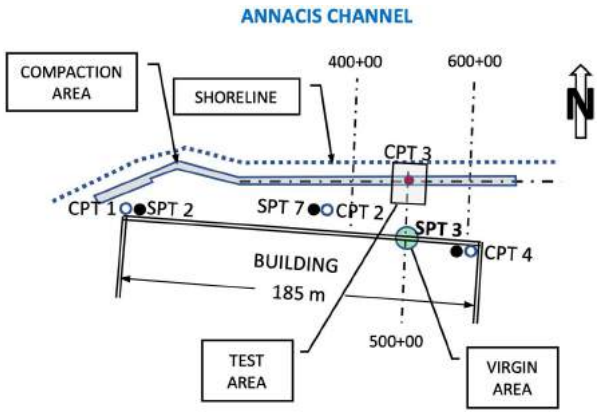

Fig. 1. Project site with location of building and area to be densified. Locations of SPT and CPT points executed prior to treatment are indicated as well as test area and virgin area for reference tests.

by Massarsch and Vanneste (1988) and Brown (1989) has been reevaluated. The project offers a unique opportunity to compare the results of the following in situ methods: (1) standard penetration test (SPT), (2) cone penetration test with pore water pressure measurement (CPTU), (3) flat dilatometer test (DMT), and lateral stress cone test (LSCPT). At the time of project execution (1988), several of these in situ methods were new in regard to both equipment and test execution, and knowledge concerning the interpretation of test data was still limited. However, with the benefit of now 30 years of experience, new insights can be obtained into the effects of vibratory compaction and in particular changes in horizontal stress.

The project involved the construction of a manufacturing storage building and a fleet-maintenance building near the Annacis Channel in British Columbia, Canada. The ground treatment work was carried out in February 1988 and required the compaction of sand down to 11 m depth. Because of the liquefaction potential of the subsoil in a strong earthquake, it was judged by the geotechnical consultant that the proposed buildings could suffer major damage. Thus, vibratory compaction was carried out along a 230-m-long, 3.0- to 4.5-m-wide area between the building site and the Annacis Channel to increase the lateral stability of the area sloping toward the Fraser River. A description of the concepts used to assess liquefaction and lateral spreading by the designer is beyond the scope of this paper. Also, this design approach may not be adequate if reevaluated based on modern methods.

Site Conditions

The site is located at the north side of Annacis Island in the upper reach and south of the Fraser River arm (Annacis Channel). A sketch of the project site showing the zone to be densified and different testing areas is shown in Fig. 1.

The site was essentially flat at an elevation of approximately 4.7 m above mean sea level. The groundwater table was affected by tidal fluctuation and was typically found 2–4 m below ground level. The geology of the Annacis Island region is typical of a tide-dominated delta. Thus, the depth and extent of different soil layers varied within a relatively short distance in the vertical and horizontal directions. Below a top crust of mixed soils was a sequence of sandy silts with seams of sand, silt, and clay, occasionally containing organic material, down to about 5 m. Below these mixed soils was a deposit of medium sand with silt and clay seams and layers, underlain at about 11.5 m depth by soft clayey silt. A borehole

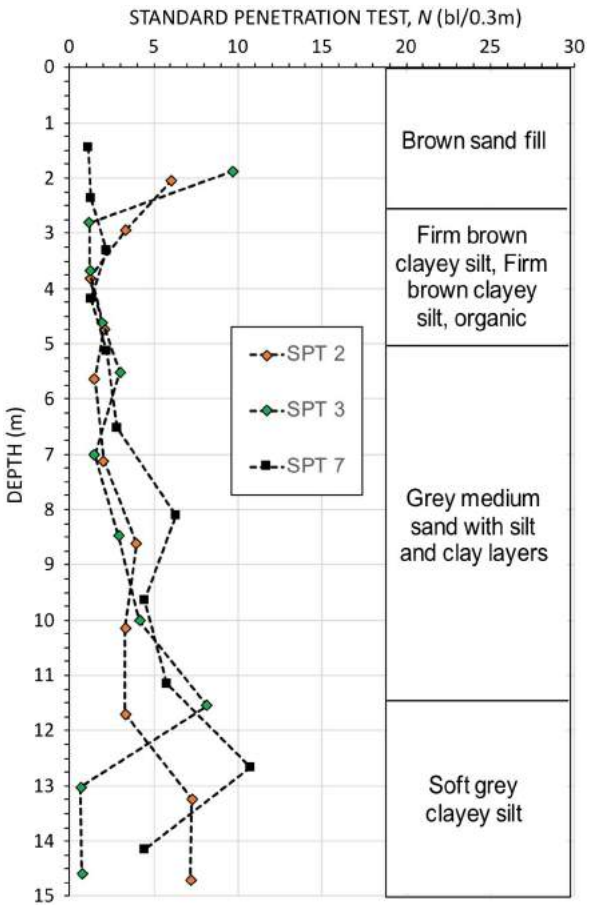

Fig. 2. Soil profile description and standard penetration tests carried out in project area prior to treatment. (Data from Massarsch and Vanneste 1988.)

description of the general soil profile at the site is given in Fig. 2. The medium sand from 5.0 to 11.5 m was judged to be susceptible to liquefaction during a strong earthquake and in need of compaction.

Penetration Tests Prior to Treatment

Fig. 2 shows the N-values (SPT 2, SPT 3, and SPT 7) from three boreholes with SPT sampling performed south of the project area (Fig. 1) before the start of the compaction work. Grain-size-distribution curves from samples of the sand layer to be densified indicated that D_{50} was about 0.3 mm, corresponding to medium sand. The SPT N-values, uncorrected with respect to the effective overburden stress, show the relative density to range from loose to medium dense.

To obtain more detailed geotechnical information, especially with respect to the existence of sandy and silty layers, which could be vulnerable to liquefaction, three CPTs (CPT 1, CPT 2, and CPT 4) were pushed in the vicinity of SPT 2, SPT 7, and SPT 3. Fig. 3 shows the distributions of cone stress, q_c, sleeve resistance, f_s, and friction ratio, R_f.

Inspection of Fig. 3 shows that CPT data provide more detailed information with respect to the soil layering than the SPT. Down to 2.5 m, layers of dense sand exist with seams or bands of sandy silt. The cone stress, q_c, is larger than 5 MPa. Between 2.5 and 5 m, the soil consists of soft silt or loose silty sand with q_c ranging from 1.5 to 3 MPa. At a depth of around 4–5 m, the soil is sand with q_c of 4–7.5 MPa. The soil types vary locally at depths. For instance,

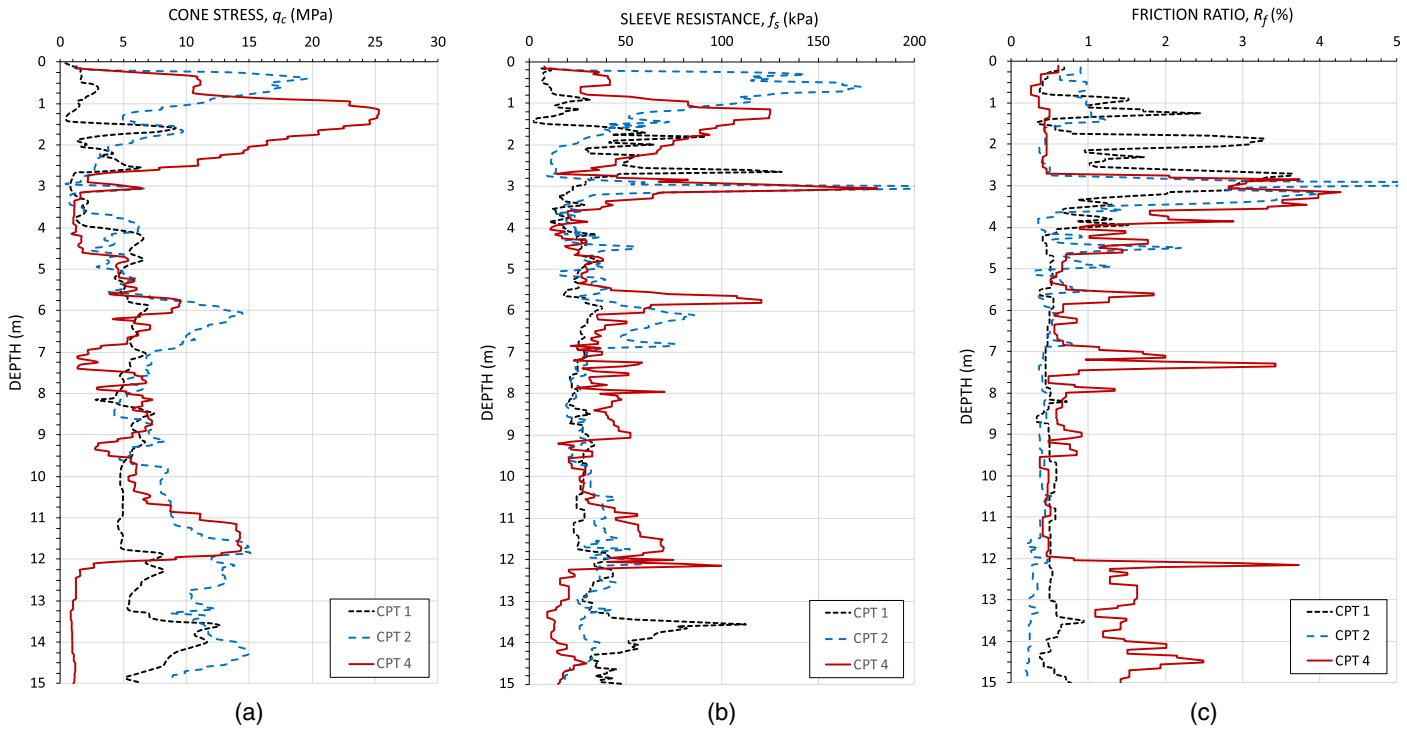

Fig. 3. Cone penetration tests in project area prior to treatment: (a) cone stress; (b) sleeve resistance; and (c) friction ratio. (Data from Massarsch and Vanneste 1988.)

between 6.5 and 7.5 m depth in CPT 4 lies an approximately 1-m-thick soft zone, as indicated by the lower cone stress (1 MPa) and higher friction ratio (2%–3%). In contrast, CPT 2, which is close to SPT 7, shows that at approximately the same depth (between 5.5 and 6.5 m) occurs, instead, a dense sand layer, where q_c is around 10–15 MPa. It is noteworthy that the sleeve resistance measured by CPT 1 is significantly lower than CPT 2 and CPT 4. The friction ratio indicates fine-grained layers, bands, or seams (silty and clayey), interbedded in the sand deposit.

Based on the detailed information obtained from the CPT, the geotechnical engineer judged the loose sand with impermeable layers and seams to be susceptible to liquefaction under the design loading conditions. Also, because these less permeable silt and clay layers affect vertical drainage, the liquefaction hazard could be enhanced. Moreover, the impeded drainage of the sand deposit, sandwiched between these layers, would also be more difficult to compact, which was the reason for the extensive testing program performed during the initial phase of vibratory compaction.

Compaction Requirements

The target SPT *N*-values after compaction were 14 at a depth of 5 m and increasing to 17 at a depth of 10 m, cf. Table 1. The liquefaction densification design of the loose to medium dense sand from 5.0 to 10 m was initially based on SPT *N*-values using a so-called donut hammer. Owing to the limitations of the SPT under the prevailing variable soil conditions and following the results of the SPT and CPT tests during the trial phase, it was decided to base the compaction requirements on CPT and a minimum cone stress, q_c, increasing from 7 MPa at a depth of 5 m to 8.5 MPa at a depth of 10 m.

The significance of interbedded layers with limited permeability on the liquefaction hazard is generally not taken into consideration in liquefaction assessment because the design assumes homogeneous soil layers. Fiegel and Kutter (1994) and Balakrishnan and Kutter (1999) reported the results of large-scale dynamic centrifuge tests of layered soil deposits subjected to base shaking. Results from the model tests involving layered soils suggest that during liquefaction, a water interlayer or very loose zone of soil develops between the sand and the silt owing to the difference in permeabilities. Soil volcanoes or boils were seen on the surface for all four of these layered model tests. Similar results from 1-g shaking table tests were reported by Kokusho (1999). The effect of layered soil deposits (sand interbedded with silt and clay) on liquefaction was also observed during full-scale compaction tests at the Annacis Island site (Massarsch and Fellenius 2017). During vibratory compaction, the loose sand between the fine-grained layers liquefied instantaneously, with the creation of sand volcanoes on the ground surface.

Table 1. Results of standard penetration tests after compaction and required *N*-index

		After compaction		
Depth (m)	Required *N*-index	DH101	DH102	DH103
1.5	—	31	25	34
3.1	—	7	8	9
4.6	14	18	16	6
6.1	16	23	23	25
7.6	16	42	39	29
9.1	17	53	65	40
10.7	—	—	27	18

Resonance Compaction Method

Because of the presence of the silt and clay layers interbedded in the sand deposit, the soil was judged marginal for vibratory compaction. The soil treatment method chosen was resonance compaction, employing the so-called Tri Star probe. The method and its

application at the Annacis Island project are described in detail by Neely and Leroy (1991), Massarsch (1991), and Massarsch and Fellenius (2017). The purpose of the resonance compaction was to densify the loose, alluvial sand. The three-bladed, 12-m-long Tri Star probe was attached to a vibrator with variable frequency (ICE 812). The compaction system was operated from a 60-t crane. The total mass of the vibrator was 6,670 kg and the eccentric moment was 46 kgm. At the maximum operating frequency of 26 Hz, the vibrator generated a 1,100-kN centrifugal force. The maximum power supplied by the power pack was 400 kW. The dynamic mass of the vibrator was 4,500 kg (including clamping but without the Tri Star probe device). The freely suspended vibrator generated a 20-mm vertical vibration movement amplitude (peak to peak). Before the start of the production work, field trials were carried out to determine the optimal spacing of compaction points and the resonance frequency. The results of the investigations are documented in detail by Massarsch and Vanneste (1988).

The resonance compaction process consisted of several phases: probe penetration at high frequency (about 25 Hz), which took approximately 2 min, followed by the compaction phase at low frequency (about 13 Hz), which typically lasted 5 min. Thereafter, the probe was withdrawn in four steps, where extraction was carried out at high frequency followed by repenetration at low frequency. The sequence of probe insertion and extraction is shown in Fig. 4.

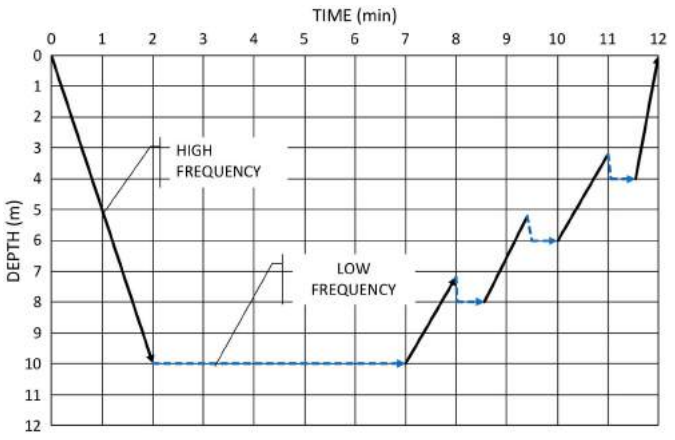

Fig. 4. Conceptual sketch of probe movement and variation of vibration frequency during resonance compaction.

The average compaction depth was 10 m, and the total time of compaction in each point was about 12 min. No material was added during compaction. The compaction equipment is shown in Fig. 5(a). The low-permeability clayey silt layer at a depth of about 3 m delayed the gradual dissipation of excess pore water pressure and caused liquefaction of the loose soil surrounding the compaction probe as shown in Fig. 5(b). During the beginning of the vibratory treatment, the soil liquefied spontaneously in some areas, confirming the liquefaction hazard of the untreated soil, as also highlighted by Massarsch and Fellenius (2017). The onset of liquefaction of the soil deposit surrounding the compaction probe could be observed by vibration measurements on the ground surface. As a result of liquefaction, ground vibrations dropped sharply and increased gradually as shaft friction along the compaction probe developed.

After compaction, the settlement was largest close to the compaction point and negligible at a distance of about 3 m. Owing to vibratory compaction, the ground surface settled by, on average, 0.30–0.45 m (Massarsch and Fellenius 2017). The depth readings of the penetration tests (CPT and DMT) performed after treatment do not account for subsidence of the ground surface, which may slightly affect a detailed comparison of test results. Extensive in situ tests were performed during compaction trials, as was monitoring of the compaction process. An important aspect of field monitoring was to develop on site the optimal compaction procedure (probe penetration sequence, duration and frequency of compaction, and grid spacing), as described by Neely and Leroy (1991) and Massarsch and Fellenius (2017). The compaction process was monitored using ground vibration measurements. In this way, it was possible to determine the time required for densification and to establish the optimal vibration frequency.

Geotechnical Investigations

Prior to the start of production work, a comprehensive field testing program was carried out to obtain more detailed information

Fig. 5. Resonance compaction and liquefaction of zone around Tri Star probe: (a) compaction equipment; and (b) manifestation of liquefaction during resonance compaction. (Reprinted from Massarsch and Vanneste 1988).

regarding the variability of soil conditions. The results of CPTs prior to, during, and after vibratory compaction were documented by Massarsch and Vanneste (1988). These data were reevaluated and used in the present paper. In addition to these tests, a comprehensive series of in situ tests was implemented by the University of British Columbia (UBC) after termination of the compaction work (Brown 1989). The UBC testing program lasted until September 1988, i.e., several months after completion of the compaction work. Two main testing areas were chosen by UBC: the test area located within the treatment area and the virgin area, as shown in Fig. 1. The tests in the compaction area were located along the centerline (C_L) at Chainage C_L 500 + 00. For comparison, tests were also carried out in the virgin area (not affected by treatment), which was located 27 m south of C_L 500 + 00, as shown in Fig. 1. Unfortunately, the soil conditions in the virgin area were not identical to those along the test area, which complicated comparison of test results. The following tests were conducted:

- cone penetration test (CPT),
- flat dilatometer test (DMT),
- seismic piezocone penetration test (SCPT), and
- lateral stress cone penetration test (LSCPT).

The results of the seismic cone penetration tests were poor owing to equipment malfunction and were therefore not included in this study. For further details, see Brown (1989). The tests were performed after compaction in two areas: within the compaction area, called the test area, and south of the compaction area, called the virgin area. The tests in the test area were located at the centerline (C_L) at the 500 foot Chainage, named C_L 500 + 00, as shown in Fig. 6. CPTs in the test area had been carried out before densification along the centerline. For details of the comprehensive testing program (and identification of different tests), see Massarsch and Vanneste (1988) and Brown (1989). Tests were performed over a period of up to 209 days (7 months) after treatment to evaluate the effect of time on the in situ test results. Due to limited space, details of the different in situ testing methods, equipment, test execution, and data interpretation per relevant standards and guidelines are not included, and only testing parameters relevant for soil compaction are considered.

CPT: A CPT reference procedure was issued by ISO (2012). The measured parameters are the cone stress, q_c, sleeve resistance, f_s, and pore water pressure, u. A derived parameter is the friction ratio, R_f.

DMT: The DMT was first introduced by Marchetti (1980). A DMT reference procedure was published by ISSMGE TC 16 (Marchetti et al. 2001). The measured parameters are two pressure readings, p_0 and p_1. The derived parameters are the material index I_D, the horizontal stress index K_D, and the dilatometer modulus E_D. Based on these three parameters, the constrained modulus, M (vertical loading), can be estimated.

LSCPT: This type of penetration test was developed by UBC primarily for research purposes. Lateral stresses are measured directly by means of a 15-cm^2 stress module located 0.75 m behind the cone tip. The lateral stress was monitored using a second friction sleeve instrumented to measure hoop stresses in a thin-walled section of the sleeve. The method has been described by Campanella et al. (1990).

Cone Penetration Tests

Cone penetration tests were performed before and at different time intervals (67 and 82 days) after treatment. The before and after compaction cone stress, q_c, sleeve resistance, f_s, and friction ratio, R_f, are shown in Fig. 7. The three CPTs show a distinct increase of both cone stress and of sleeve resistance following compaction. The friction ratio demonstrates soil stratification with several fine-grained soil layers (friction ratio exceeding 1%). The measurements are influenced by the occurrence of silty and clayey layers, in particular between depths of 3 and 4 m. The improvement of q_c is less pronounced in the silty and clayey layers (at depths of 4, 5.5, and 7.5 m). It is apparent that both the cone stress and the sleeve resistance have increased in the compacted sand. Between depths of 5 and 10 m, the cone stress and the sleeve resistance increased on average by a factor of two to four, almost independently of time after treatment (62 and 82 days, respectively). Fig. 7(c) shows the friction ratio, R_f, before treatment and 67 and 82 days after treatment. It is interesting to note that the friction ratio apparently decreased after treatment. Brown (1989) drew the conclusion that the soil had become more coarse-grained due to mixing as a result of vibratory compaction. In the opinion of the authors, this conclusion is not supported by the results. Rather, the change in friction ratio is

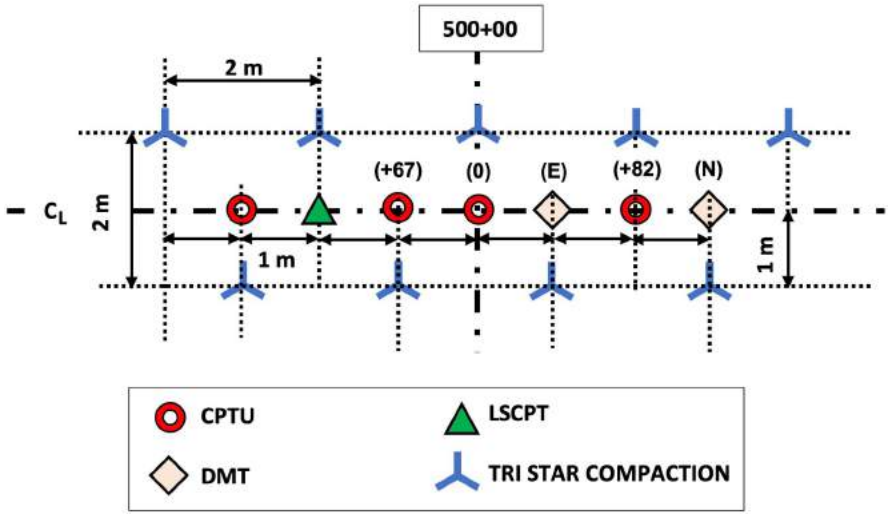

Fig. 6. Location of compaction points in test area C_L 500 + 00. The time after compaction (CPT: days) and the measuring direction (DMT: east, north) are shown in brackets.

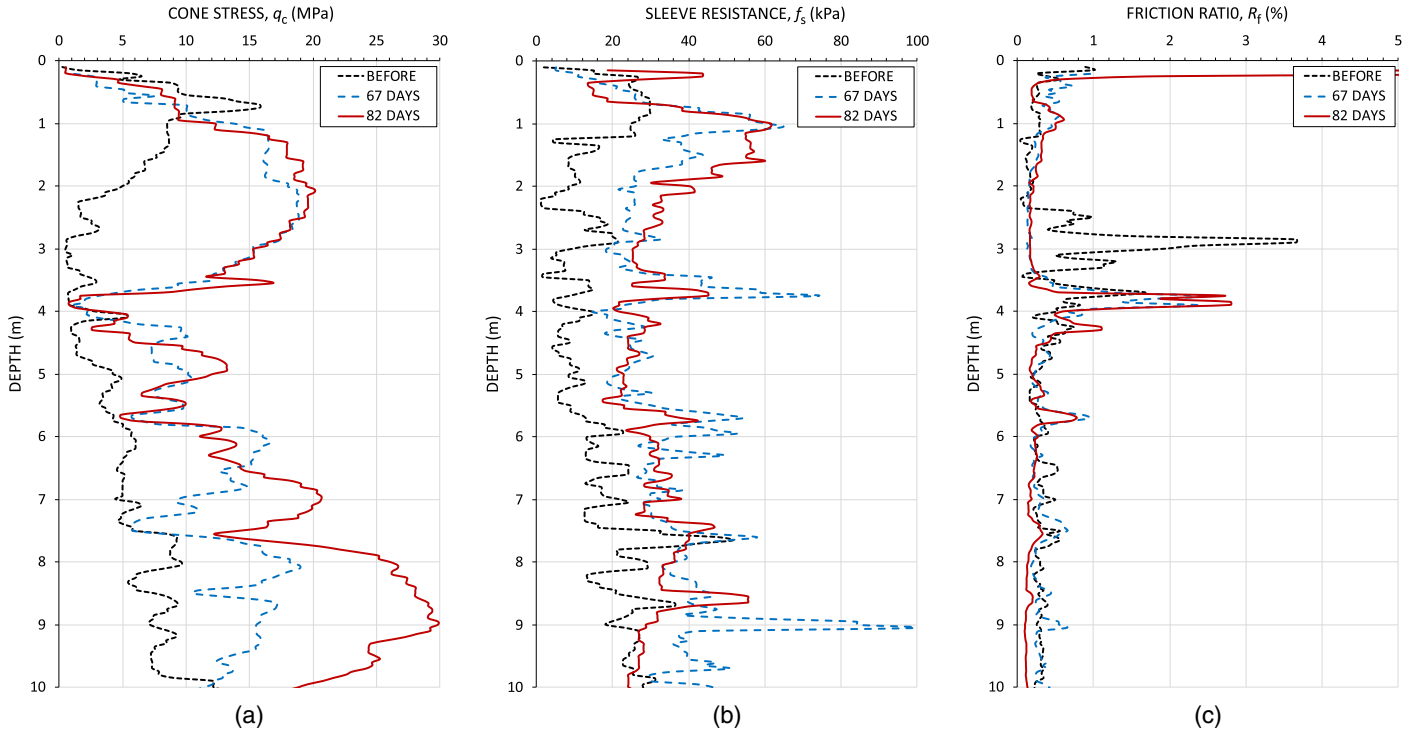

Fig. 7. Results of CPT before and at 67 and 82 days after treatment: (a) cone stress; (b) sleeve resistance; and (c) friction ratio.

due to the change in horizontal stress induced by the compaction. This effect was also observed by Howie et al. (2000) and Nguyen et al. (2014). A change in horizontal stress influences sleeve resistance and can result in a corresponding decrease of apparent fines content. To account for this effect, Nguyen et al. (2014) proposed a correction method to maintain the same fines content in the pre- and posttreatment CPT-based liquefaction analyses.

Fig. 8(a) plots the cone stress, q_c (logarithmic scale), against the friction ratio, R_f (linear scale), in the soil-type evaluation introduced by Robertson et al. (1986), known as a soil behavior type (SBT) chart. Note that, according to Fig. 7(c), the friction ratio decreased following compaction. However, this is a consequence of the fact that the sleeve resistance increased less than the cone stress. The change of cone stress and sleeve resistance is even more clear when plotting the before and after compaction data according to the Eslami–Fellenius soil classification chart (Fellenius and Eslami 2000), which displays cone stress versus sleeve resistance directly, as shown in Fig. 8(b) (in linear scales). Comparison of Figs. 8(a and b) demonstrates the advantages of the simpler q_c versus f_s chart, visualizing clearly the change of sleeve resistance as a result of soil compaction. Therefore, the authors recommend presenting the results of soil compaction projects not only as a SBT chart but also in a simple cone stress versus sleeve resistance diagram, which more clearly reflects the effects of soil compaction.

Flat Dilatometer Test

The DMT was performed 111 days after treatment at several locations with slightly variable soil conditions. The time of testing was dictated by equipment availability and site access. One test was performed in the virgin area and two tests in the test area at the centerline between compaction points, with one test where the blade was facing east (E) and the other where the blade was facing north (N) (Fig. 6). For details of the test evaluation procedure, see Marchetti et al. (2001).

The interpreted material index, I_D, shown in Fig. 9, is related to soil type, according to the following classification: (1) clay $0.1 < I_D < 0.6$, (2) silt $0.6 < I_D < 1.8$, and (3) sand $1.8 < I_D < 10$. The soil classification according to the DMT agrees with the soil type based on the friction ratio from the CPT shown in Fig. 8. I_D ranges generally between 1 and 3, with the exception of lower values (0.1 to 1.0) in the several clay and silt layers. Marchetti et al. (2001) determined a dilatometer modulus, E_D, from the DMT pressure readings (p_0 and p_1). The dilatometer modulus prior to compaction in the virgin area is shown in Fig. 10. These measurements are compared with the results in the test area 111 days after treatment. Note that the soil layer profile differed somewhat between the test area and virgin area. The dilatometer modulus, E_D, shows low values in the virgin area due to a fine-grained zone between 2 and 3.5 m. Similar soft areas were detected at depths of 3.5 and approximately 6.5 m in the test area. It can be seen that in the test area between depths of 6 and 10 m, E_D increased by a factor of 2–3.5. The large increase between 2 and 3 m is due to the soft layer in the virgin area. There is no significant difference between the measurements in the two directions (blade facing east and north, respectively).

The constrained modulus, M, can be determined based on E_D measurements shown in Fig. 10. The following conversion procedure was proposed by Marchetti et al. (2001):

$$M = R_M E_D \tag{1}$$

For $0.6 < I_D < 3$, the following relationships were proposed:

$$R_M = R_{M0} + (2.5 - R_{M0}) \log K_D \tag{2}$$

$$R_{M0} = 0.14 + 0.15(I_D - 0.6) \tag{3}$$

The distribution of the constrained modulus, M (test area, 111 days after compaction compared with the M from the virgin

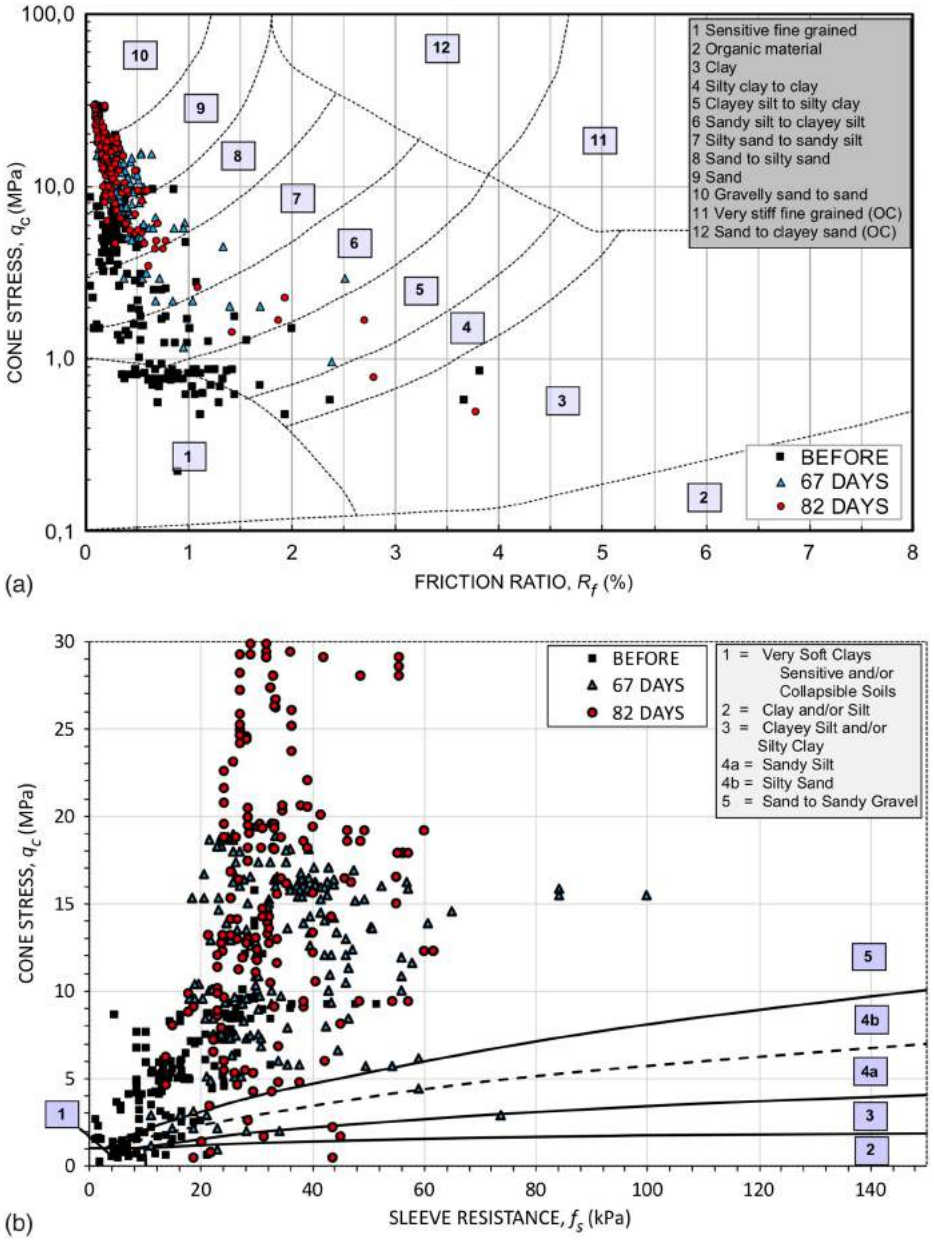

Fig. 8. Soil classification using CPT results shown in Fig. 7: (a) SBT chart (data from Robertson and Campanella 1983); and (b) classification according to Fellenius and Eslami (2000), showing cone stress as function of sleeve resistance, both in linear scale.

area test before compaction), can be calculated and is shown in Fig. 11. Again, due to the variability in the upper 6 m of soil, only the improvement in the lower part of the sand deposit (6–9 m) is of relevance. In this zone, the constrained modulus increased by a factor of 2–3.5. An important consequence of the vibratory compaction of sand is the change of horizontal stress. From the DMT, the horizontal stress index, K_D, can be determined according to the procedure recommended by Marchetti et al. (2001). The results are shown in Fig. 12. It should be noted that in the virgin area, the upper soil layer was very stiff but below 2–4 m followed soft silty and clayey layers, which affected the comparison of K_D values. The DMT 111N had to be terminated at 8.5 m depth for operational reasons. Neglecting the upper 6 m of variable soil layers, there is a noticeable increase of K_D in the compacted sand in the depth interval of 6–9 m. On average, K_D increased as a result of compaction by a factor of 1.5–2.5.

Lateral Stress Cone Penetration Test

Lateral stress cone penetration tests were carried out 204 days after compaction, as well as in the virgin area; hence, time effects are subject to uncertainty. The LSCPT is of particular interest when assessing horizontal stress changes and to compare these with other measurements, such as sleeve resistance (CPT) and horizontal stress index (DMT). The LSCPT program involved one test on the centerline of vibrocompaction at Chainage 500 + 00, 204 days after treatment, and one test in the virgin area (209 days after treatment) (Fig. 6).

Lateral stresses were measured by means of a measurement module, located 0.75 m behind the cone tip. The measured horizontal stresses were affected by soil disturbance during the penetration test. Also, the cylindrical shape changed the stress distribution. To determine the true in situ stresses, the effect of stress change due

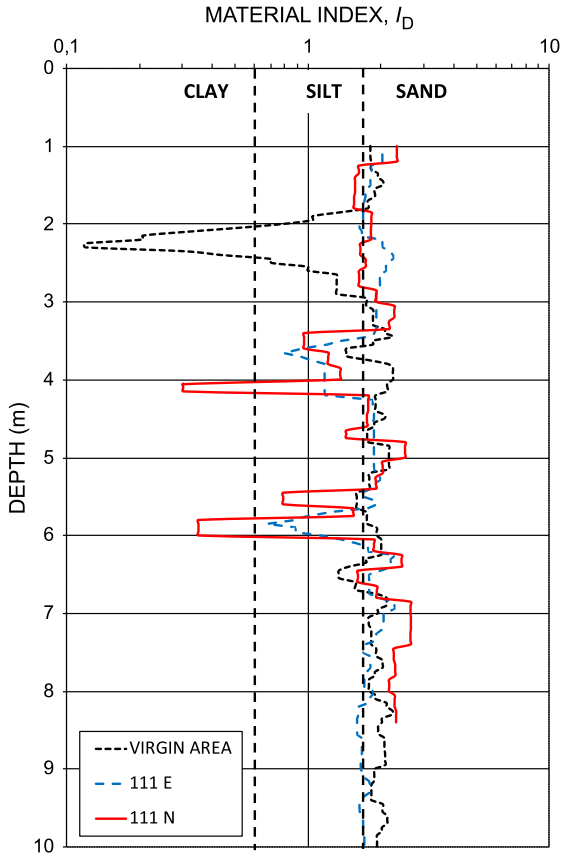

Fig. 9. Variation of material index, I_D, with depth. Material boundaries are indicated according to Marchetti et al. (2001). Tests in virgin area and adjacent to compaction point with blade facing north (N) and east (E), respectively.

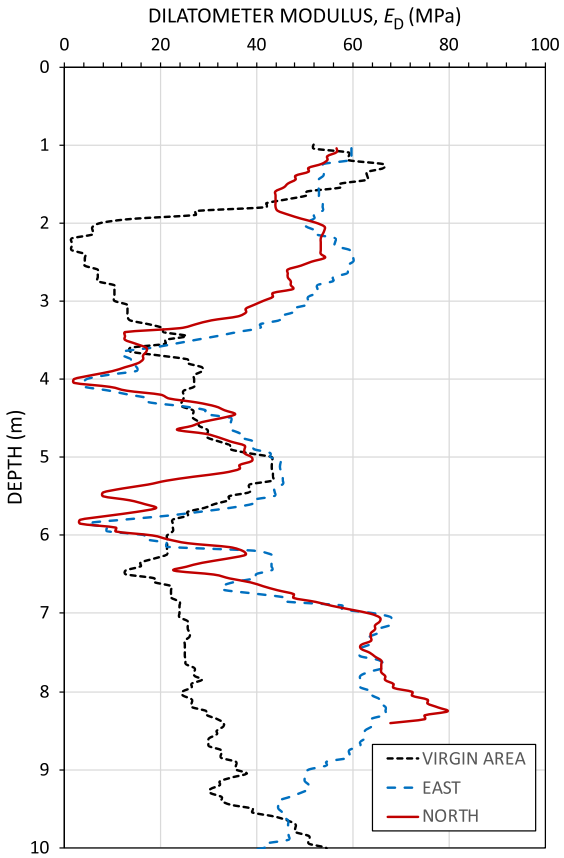

Fig. 10. Dilatometer modulus, E_D, for virgin area before compaction and for test area 111 days after compaction for two blade orientations (facing east and north).

to displacement had to be evaluated. However, in this study, the change in horizontal stress from before treatment to that after treatment is the interesting aspect; the disturbance effect can therefore be neglected. The profile of measured lateral stress versus depth is shown in Fig. 13. Unfortunately, the different soil conditions in the virgin area and the test area make it difficult to provide a fully representative comparison. It is interesting to compare the lateral stress measured by the LSCPT with the K_D values obtained from the DMT (Fig. 12). As can be seen, there is reasonable agreement between the increase in the horizontal stress index, K_D, from the DMT and the lateral stress measured by the LSCPT. Thus, this information supports the assumption that vibratory compaction of sand without the introduction of additional material (vibroreplacement, compaction grouting, or displacement piles) causes a permanent increase in horizontal stress.

Overconsolidation Ratio

The overconsolidation ratio (OCR) is an important design parameter for settlement analyses but also for the assessment of the liquefaction hazard. Massarsch and Fellenius (2002) described the results of comprehensive CPT investigations in connection with the compaction of a sand fill, where sleeve resistance increased by about the same ratio as cone stress. They presented a simplified concept of how the increase in horizontal stress (based on the ratio of sleeve resistance after compaction to that before) could be used to estimate OCR. Although some uncertainty exists regarding the accuracy of the measured sleeve resistance, the relative increase in sleeve resistance (determined from the ratio of sleeve resistance values after compaction with values before compaction) can be considered a reliable indicator of changes in horizontal stress (Robertson 2016). Based on results of laboratory compression chamber tests, several investigators (Schmertmann 1985; Mayne and Kulhawy 1982; Jamiolkowski et al. 1988) have proposed an empirical relationship between the earth stress coefficient of normally consolidated sand, K_0, and that of overconsolidated sand, K_1, as expressed in Eqs. (4) and (5).

$$\frac{K_1}{K_0} = \mathrm{OCR}^{\beta} \tag{4}$$

$$\mathrm{OCR} = \left[\frac{K_1}{K_0}\right]^{\frac{1}{\beta}} \tag{5}$$

where K_0 = coefficient of earth stress at rest for normally consolidated sand; K_1 = coefficient of earth stress at rest for overconsolidated sand; and β = empirically determined exponent.

Based on the evaluation of calibration chamber tests using DMTs reported by Lee et al. (2011), Massarsch and Fellenius (2019) recommended a value of $\beta = 0.48$.

OCR Based on Cone Stress

In a recent paper, Mayne and Styler (2018) presented a simple concept to estimate the preconsolidation stress (yield stress), σ'_p, and OCR based on CPT. For so-called well-behaved soils, the effective yield stress can be expressed by the following simple expression:

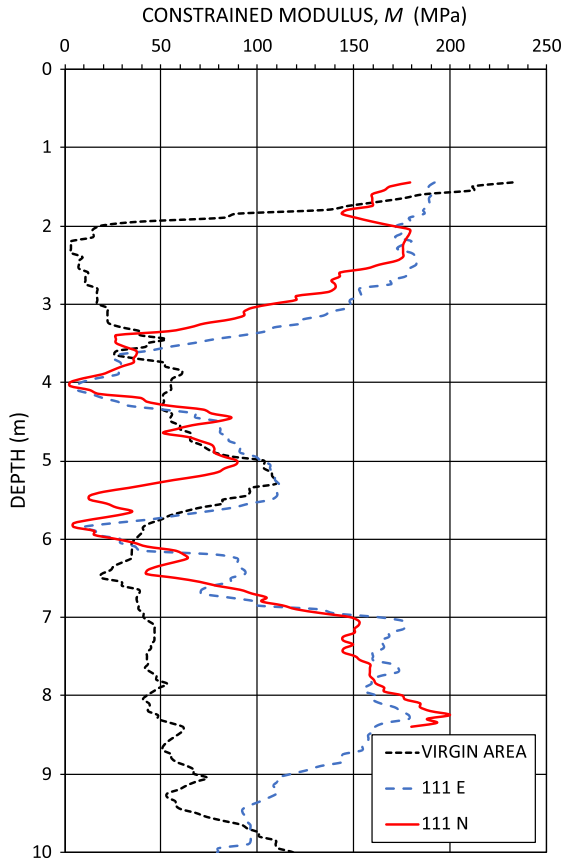

Fig. 11. Constrained modulus, M, determined from dilatometer modulus, E_D, for virgin area before compaction and for test area 111 days after compaction.

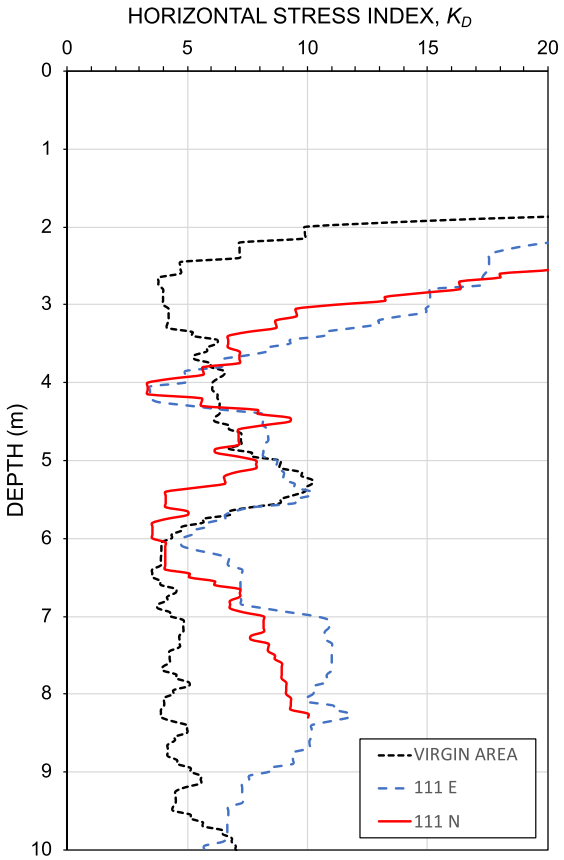

Fig. 12. Horizontal stress index, K_D, as function of depth for virgin area before compaction and for test area 111 days after compaction.

$$\sigma_p' = 0.33(q_{\text{net}})^{m'}\left(\frac{\sigma_r}{100}\right)^{(1-m')} \tag{6}$$

where q_{net} = net cone stress, $q_t - \sigma_{vo}$; and m' = empirical yield stress exponent (Table 2). The term σ_r is the reference stress equal to atmospheric pressure (100 kPa). Based on Eq. (6) and choosing the yield stress exponent, m', according to the soil type suggested in Table 2, the yield stress, σ_p', and the overconsolidation ratio, OCR, can be determined. The variation of the preconsolidation stress and overconsolidation ratio in the sand layer between depths of 5 and 10 m is shown in Figs. 14(a and b), respectively. Fig. 14 suggests that the sand deposit was already preconsolidated before compaction (OCR $\approx$ 2.5) and the OCR increased following compaction to between 3 and 6. Because the CPT soundings were performed in the same testing area before and after compaction, the sleeve resistance, f_s, can be used to estimate the OCR according to Eq. (5). The variation of OCR with depth for two time instances (67 and 82 days after treatment) is shown in Fig. 15(a). The diagram indicates a definite increase in OCR throughout the treated soil layer, in spite of some variations due to soil layering, as has been discussed above. In the opinion of the authors, the slightly lower OCR after 82 days, compared to the value after 67 days, reflects the variability of the soil conditions rather than stress relaxation. The increase in the OCR is most pronounced in the upper soil deposit that contains layers of silt and clay. In the sand below about 6 m, the increase in the OCR is almost constant with depth, ranging between 2 and 5. This increase in the OCR—and thus of preconsolidation stress—is significant for settlement analysis and liquefaction assessment.

OCR Based on Horizontal Stress Index

The horizontal stress index, K_D, can be considered a reliable method for detecting changes in horizontal stress. In the present case, the DMT measurements performed in the test area 204 days after treatment were compared with the measurements in the virgin area. However, the soil conditions in the two areas differed somewhat, especially in the upper layers, which affects the validity of comparison. The OCR determined according to Eq. (5) is shown in Fig. 15(b), using the K_D ratio (after compaction/before compaction). Most reliable for comparison are the OCR data in the compacted sand layer below 6 m, where the OCR ranges between 2 and 7, with an average of 5. This range of OCR values is in reasonable agreement with the previously shown results based on sleeve resistance measurements.

It should be pointed out that the comparison of DMT measurements between the test area and the virgin area is uncertain, but nevertheless the increase of horizontal stress is an indication of the increase of the overconsolidation ratio.

Determination of Constrained Modulus

Soil compaction is frequently required to reduce total and differential settlement. For settlement analyses, the tangent modulus method described by Janbu (1985) is recommended. The concept

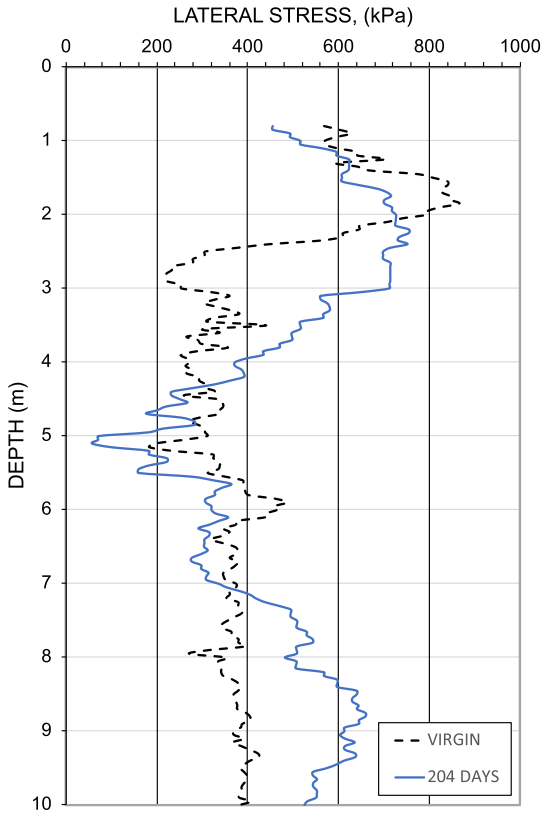

Fig. 13. Lateral stress measurement in virgin area and in test area 204 days after compaction.

Table 2. Yield stress exponent, m' for different soil types

Soil type	Yield stress exponent, m′
Fissured clays	1.1
Organic clays	0.9
Silty sands	0.80
Intact clays	1.0
Silt mixtures	0.85
Clean sands	0.72

Source: Data from Mayne and Styler (2018).

is outlined in detail in the Canadian Foundation Engineering Manual (CFEM 1985, 1992). For settlement analyses, the correct assumption of the constrained modulus is essential. However, the constrained modulus is generally nonlinear and stress dependent, an effect that needs to be taken into consideration. The tangent modulus, M, is defined by the following relationship:

$$M = \frac{d\sigma}{d\varepsilon} = m\sigma_r \left(\frac{\sigma_v'}{\sigma_r}\right)^{(1-j)} \tag{7}$$

where $d\sigma$ = change of stress; $d\varepsilon$ = change of strain; m = modulus number (dimensionless); σ_r = reference stress (equal to 100 kPa); σ_v' = vertical effective stress; and j = stress exponent. For uncompacted sand, a stress exponent of $j = 0.5$ can be assumed. For compacted sand, which behaves essentially as an elastic material, the stress exponent should be increased to $j = 1$ (Janbu 1985). The following relationship for estimating the modulus number, m, from the constrained modulus, M, can be used:

$$m = \frac{M}{\sigma_r}\left(\frac{\sigma_v'}{\sigma_r}\right)^{j-1} \tag{8}$$

For the case of normally consolidated sand, where $j = 0.5$ can be assumed, the modulus number, m, is obtained from

$$m = M\left(\frac{1}{\sigma_r \sigma_v'}\right)^{0.5} \tag{9}$$

For the case of compacted sand, where $j = 1$ can be assumed, the following simple relationship is obtained:

$$m = \frac{M}{\sigma_r} \tag{10}$$

Thus, for compacted sand, the modulus number m can be determined by dividing M (in kPa) by 100 (reference stress, σ_r). Empirical values have been reported in the literature, and typical values of the modulus number are given by CFEM (1985, 1992) (Table 3).

It can be seen that for loose to compact sand, which would correspond to sand prior to treatment, m ranges from 100 to about 250. Similar values of the modulus number for normally consolidated soils have been reported by Janbu (1985). For dense sand after compaction, m can be assumed to fall in the range 250–400. However, it is possible that the modulus number for vibratory compacted sand could be significantly higher due the preconsolidation effect caused by multiple reloading cycles.

Based on the values given in Table 3 it is possible to backcalculate for CPT and DMT, from the previously determined constrained modulus, M (CPT and DMT), the equivalent modulus number, m.

Constrained Modulus from CPT

Massarsch (1994) proposed a concept to estimate the modulus number from CPT. A stress adjustment factor, C_M is used to adjust the measured cone stress, q_c, with respect to the mean effective stress:

$$C_M = \left(\frac{\sigma_r}{\sigma_m'}\right)^{0.5} \tag{11}$$

where C_M = stress adjustment factor ≤ 2.5; σ_r = reference stress = 100 kPa; and σ_m' = mean effective stress. Note that at $\sigma_m' = 100$ kPa, $C_M = 1$; thus, the stress adjustment converts the measured cone stress, q_c, to an equivalent value at 100 kPa mean effective stress.

As was demonstrated earlier, horizontal stresses increase during soil compaction, and this aspect needs to be considered when correcting the cone stress. Therefore, an important aspect in the case of soil compaction is that the mean effective stress is used for normalization of the cone stress instead of the more commonly used vertical effective stress. The so adjusted cone stress, q_{CM}, can be considered independent of stress (and thus depth), reflecting fundamental soil behavior, such as strength and stiffness:

$$q_{cM} = q_c C_M = q_c \left(\frac{\sigma_r}{\sigma_m'}\right)^{0.5} \tag{12}$$

Massarsch and Fellenius (2002) proposed that for granular soils, the modulus number, m, can be correlated to the stress-adjusted cone stress, q_{cM}:

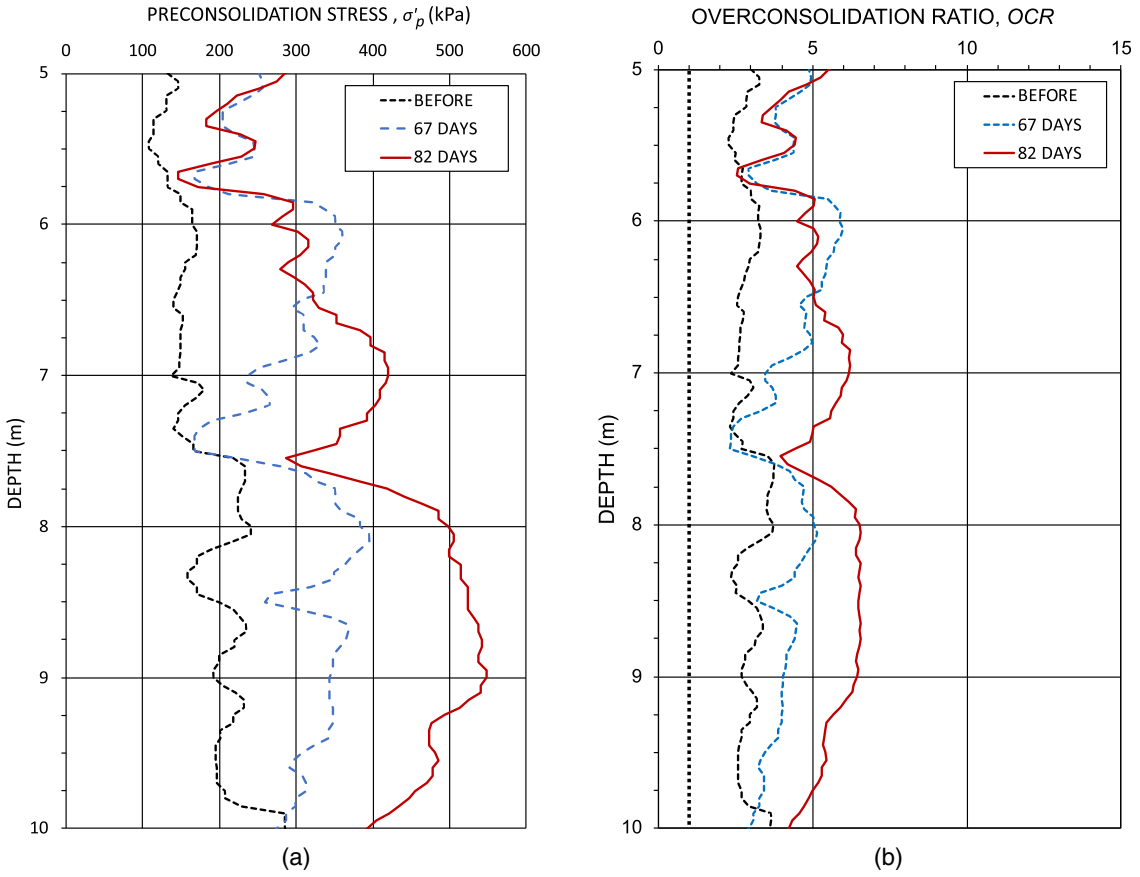

Fig. 14. (a) Preconsolidation stress; and (b) overconsolidation ratio determined according to Eq. (6) in sand layer between 5 and 10 m depth ($m' = 0.72$).

$$m = a\left(\frac{q_{cM}}{\sigma_r}\right)^{0.5} \tag{13}$$

where m = modulus number; a = empirical modulus factor that depends on soil type; q_{cM} = stress-adjusted cone stress; and σ_r = reference stress = 100 kPa. The modulus factor, a, was determined based on experience from soil compaction projects. Typical values of a are given in Table 4.

Modulus Number from CPT

The mean effective stress must be estimated for the calculation of the q_{cM} according to Eq. (12). The following average values were chosen: for loose sand, $K_0 = 0.40$–0.50 and $j = 0.5$; for compacted sand, $K_0 = 1.0$ and $j = 1$, respectively. The cone stress determined prior to treatment and at two time intervals after compaction (67 and 82 days) was used to calculate the range of the modulus number by the foregoing relations. The modulus number is determined from Eq. (12) and Table 4, assuming $a = 28$ in the upper dense layer, $a = 20$ for the loose sand prior to compaction, and $a = 35$ after compaction (dense sand).

The modulus number as a function of depth is shown in Fig. 16(a). Before compaction, the modulus number ranged between 80 (silty sand) and 220 (sand), with the exception of the dense upper soil layer, where the modulus numbers ranged between 500 and 700. The modulus number increased markedly following compaction. In the sand layer below 6 m, the average modulus number increased to between 300 and 450. This range of values is in good agreement with the empirical values proposed for dense sand. It should be pointed out that the method of estimating the modulus number based on cone stress was derived based on the empirical m values given in Table 3 without considering the effect of horizontal stress changes.

Modulus Number from DMT

Based upon Eq. (9), the modulus number was calculated from the derived constrained modulus, M, shown in Fig. 11. The variation of the modulus number as a function of depth is presented in Fig. 11(b) in the virgin area and the test area 111 days after treatment (east and north). A comparison of the modulus number derived from CPT and DMT shows that the modulus number based on q_c is in good agreement with the empirical values shown in Table 3. The modulus number determined from the constrained modulus measured by the DMT can be compared with typical values according to Fig. 16(b). The upper range for the modulus number for uncompacted sand is about $m = 200$ and for dense compacted sand $m = 400$. The values of modulus number, m, based on the constrained modulus, M, determined from the DMT are significantly higher than the values given in Table 3. Massarsch and Fellenius (2019) have shown that in overconsolidated (compacted) sand, the constrained modulus determined from the DMT can be significantly higher than values based on normally consolidated conditions. However, it is important to point out that the DMT measures soil properties in the horizontal direction, and thus takes into account the effect of stress increase and overconsolidation achieved by vibratory compaction.

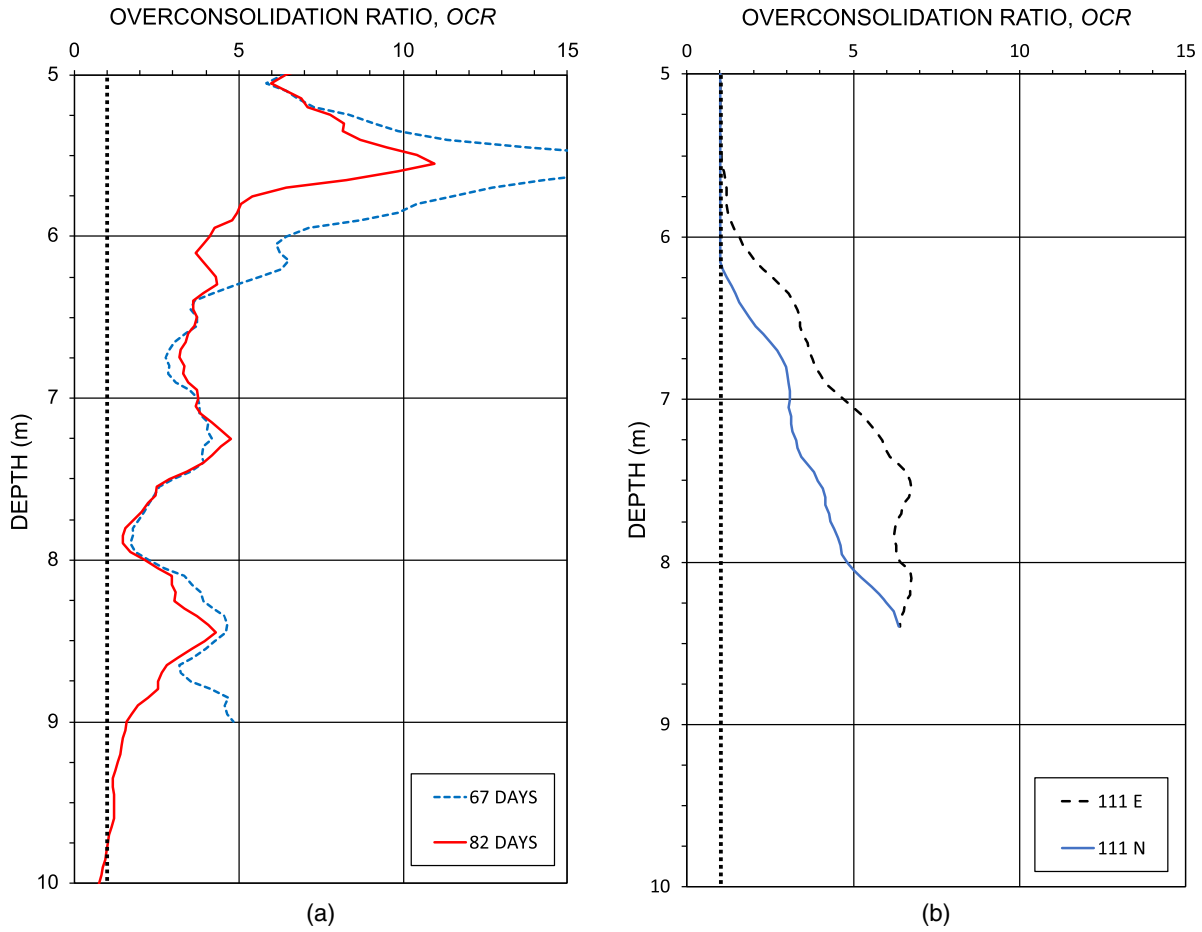

Fig. 15. OCR determined from (a) CPT, sleeve resistance, f_s; and (b) DMT, horizontal stress index, K_D.

Table 3. Typical stress exponent and modulus numbers for granular soils

Soil type	Stress exponent, j	Range, m	Average, m
Till, very dense to dense	1	1,000–300	650
Gravel	1	400–40	220
Sand			
Dense	1	400–250	325
Compact	1	250–150	200
Loose	0.5	150–100	125
Silt			
Dense	1	200–80	140
Compact	1	80–60	70
Loose	0.5	60–40	50

Sources: Data from CFEM (1985, 1992).

Table 4. Modulus factor, a, for different soil types

Soil type	Modulus factor, a
Silt, organic soft	7
Silt, loose	12
Silt, compact	15
Silt, dense	20
Sand, silty loose	20
Sand, loose	22
Sand, compact	28
Sand, dense	35
Gravel, loose	35
Gravel, compact	40
Gravel, dense	45

Source: Data from Massarsch and Fellenius (2002).

Conclusions

The effects of vibratory compaction (resonance compaction method) in a natural soil deposit were investigated. The soil deposit consisted of sand from depths of approximately 6 to 10 m overlain by layers of silty and clayey sand and silt. Vibratory compaction was chosen to mitigate the liquefaction hazard. During the initial phase of resonance compaction, the soil surrounding the compaction probe liquefied and groundwater emerged at the ground surface.

Different types of in situ tests (SPT, CPT, DMT, and LSCPT) were performed. As a result of vibratory compaction, all measured soil parameters (cone stress, sleeve resistance, horizontal stress index) increased. An important aspect of this study was to investigate the effect of vibratory compaction (without the introduction of additional material) on horizontal stress, in addition to the expected increase in cone stress. Measurements of sleeve resistance (CPT), horizontal stress (LSCPT), and horizontal stress index (DMT) showed a significant increase as a result of compaction.

The overconsolidation ratio was estimated by different methods. In spite of the variable soil conditions, it can be concluded that vibratory compaction causes preconsolidation and thus an increase in OCR. This frequently neglected effect should be considered in geotechnical design, such as in settlement analyses or liquefaction hazard assessment.

The constrained modulus and the modulus number of the uncompacted soil, estimated from the CPT and DMT, are in agreement with empirical data. After compaction, the modulus number increases significantly. The constrained modulus determined from the CPT gives values in agreement with empirical data (based on

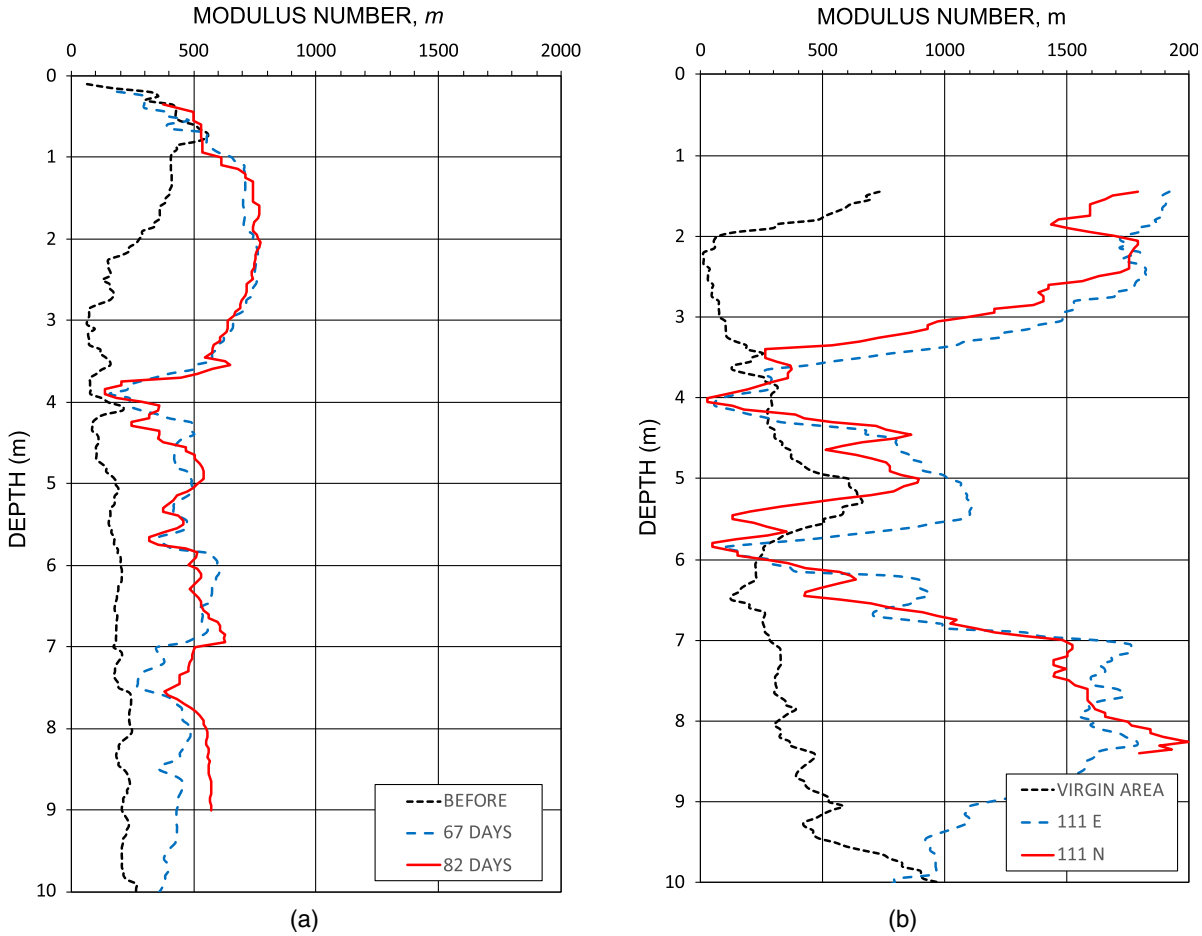

Fig. 16. Variation of modulus number, m, as function of depth: (a) determined from CPT, cf. Fig. 7(a); and (b) determined from DMT, Fig. 11.

investigation of normally consolidated soils), while the constrained modulus derived from the DMT gives significantly higher values. These higher values of the constrained modulus could be explained by the fact that the DMT reflects the change in horizontal stress and overconsolidation.

Although the results of one method of vibratory compaction (resonance compaction) have been studied, it is believed that the compaction effect is largely the same for all vibratory compaction methods: soil is compacted and becomes overconsolidated, and the horizontal stresses increase as a result.

Acknowledgments

The first author is indebted to the important contributions of the geotechnical department of the University of British Columbia (UBC) and in particular to Prof. R. Campanella and Mr. David F. Brown for the diligence with which the field investigations were carried out. The Tri Star resonance compaction work was managed by Mr. Leroy and supervised by Mr. Vanneste. Finally, the authors wish to acknowledge the effort and important comments made by two of the reviewers. Their contributions helped to improve the quality of the paper.

Notation

The following symbols are used in this paper:

a = empirical modulus factor;
C_L = centerline;
C_M = stress adjustment factor;
$d\varepsilon$ = change of strain;
$d\sigma$ = change of stress;
E_D = dilatometer modulus;
fs = sleeve resistance;
I_D = material index;
j = stress exponent;
K_0 = coefficient of earth stress at rest for normally consolidated soil;
K_1 = coefficient of earth stress at rest for overconsolidated soil;
K_D = horizontal stress index (flat dilatometer test);
M = constrained modulus, tangent modulus;
m = modulus number;
m' = yield stress exponent;
N = uncorrected standard penetration test index;
q_c = cone stress;
q_{CM} = adjusted cone stress;
R_f = friction ratio;
R_M = modulus correction factor (flat dilatometer test);
R_{M0} = correction factor of R_M (flat dilatometer test);
u_0 = equilibrium pore pressure;
β = empirically determined exponent for OCR;
σ'_m = mean effective stress;
σ_r = reference stress (equal to 100 kPa); and
σ'_v = vertical effective stress.

References

Asalemi, A.A., 2006. Application of seismic cone for characterization of ground improved by vibro-replacement. Ph.D. thesis, Geotechnical Engineering, Univ. of British Columbia.

Balakrishnan, A., and Kutter. B.L. 1999. Settlement, sliding, and liquefaction remediation of layered soil. *J. Geotech. Geoenviron. Eng.* 125 (11): 968–978. https://doi.org/10.1061/(ASCE)1090-0241(1999)125:11(968).

Brown, D.F., 1989. Evaluation of the Tri Star vibrocompaction probe. Master thesis, Dept. of Civil Engineering, Univ. of British Columbia.

Campanella, R.G., Sully, J.P., Grieg, J., and Jolly, G., 1990. Research and development of a lateral stress piezocone. *Transp. Res. Rec.* 1278: 215–224.

CFEM (Canadian Foundation Engineering Manual). 1985. *Canadian geotechnical*, 2nd ed. Richmond, BC: BiTech Publishers.

CFEM (Canadian Foundation Engineering Manual). 1992. *Canadian geotechnical*, 3rd ed. Richmond, BC: BiTech Publishers.

Fellenius, B.H., and Eslami, A., 2000. Soil profile interpreted from CPTU data. In Vol. 1 of *Proc., Year 2000 Geotechnics Conf. Southeast Asian Geotechnical Society*, edited by A.S. Balasubramaniam, D.T. Bergado, L. Der Gyey, T.H. Seah, K. Miura, N. Phien wej, and P. Nutalaya, 163-171. Bangkok, Thailand: Asian Institute of Technology.

Fiegel, G.L., and Kutter, B.L., 1994. Liquefaction-induced lateral spreading of mildly sloping ground. *J. Eng. Geol.* 120 (12): 2236–2243. https://doi.org/10.1061/(ASCE)0733-9410(1994)120:12(2236).

Howie, J.A., Daniel, C., Asalemi, A.A., and Campanella, R.G., 2000. Combinations of in situ tests for control of ground modification in silts and sands. In *Geo-Denver 2000, Innovations and Applications in Geotechnical Site Characterization*, edited by P.W. Mayne and R. Hryciw. Reston, VA: ASCE.

ISO. 2012. *Geotechnical investigation and testing—Field testing—Part 1: Electrical cone and piezocone penetration test*. ISO 22476-1:2012. Geneva: ISO.

Jamiolkowski, M., Ghionna, V.N., Lancelotta, R., and Pasqualini, E., 1988. New correlations of penetration tests for design practice. In *Proc., 1st Int. Symp. on Penetration Testing*, edited by J. DeRuiter, 263–296. Rotterdam, Netherlands: A.A. Balkema.

Janbu, N. 1985. Soil models in offshore engineering. *Geotechnique* 35 (3): 241–281. https://doi.org/10.1680/geot.1985.35.3.241.

Kokusho, T. 1999. Water film in liquefied sand and its effect on lateral spread. *J. Geotech. Geoenviron. Eng.* 125 (10): 817–826. https://doi.org/10.1061/(ASCE)1090-0241(1999)125:10(817).

Lee, M., Choi, S., Kim, M., and Lee, W., 2011. Effect of stress history on CPT and DMT results in sand. *J. Eng. Geol.* 117 (3–4): 259–265. https://doi.org/10.1016/j.enggeo.2010.11.005.

Marchetti, S. 1980. In situ tests by flat dilatometer. *J. Geotech. Eng. Div.* 106 (GT3): 299–321.

Marchetti, S., Monaco, P., Totani, G., and Calabrese, M., 2001. The flat dilatometer test (DMT) in soil investigations. In *Proc., In Situ 2001, Int. Conf. on In Situ Measurement of Soil Properties*, pp. 8-48.

Massarsch, K.R., 1991. Deep soil compaction using vibratory probes. In *Proc., ASTM Symp. on Design, Construction and Testing of Deep Foundation Improvement: Stone Columns and Related Techniques*, edited by R. C. Bachus, 297–319. West Conshohocken, PA: ASTM.

Massarsch, K.R., 1994. Settlement analysis of compacted fill. In *Proc., 13th Int. Conf. on Soil Mechanics and Foundation Engineering*, 325–328. Boca Raton, FL: CRC Press.

Massarsch, K.R. and Fellenius, B.H., 2002. Vibratory compaction of coarse-grained soils. *Can. Geotech. J.* 39 (3): 695–709. https://doi.org/10.1139/t02-006.

Massarsch, K.R., andFellenius, B.H., 2017. Liquefaction assessment by full-scale vibratory testing. In *Proc., 70th Annual Canadian Geotechnical Conf.*, 7. Richmond, BC: Canadian Geotechnical Society.

Massarsch, K.R., and Fellenius, B.H., 2019. In situ tests for settlement design of compacted sand. *Proc. Inst. Civ. Eng. Geotech. Eng.* 172 (3): 207–217. https://doi.org/10.1680/jgeen.18.00046.

Massarsch, K. R. and G. Vanneste, G., 1988. *TriStar vibrocompaction Annacis Island*. FIT Rep. Liege, Belgium: Franki International.

Mayne, P.W., and Kulhawy, F.H., 1982. K_0-OCR relationship in soil. *J. Geotech. Eng.* 108 (6): 851–872.

Mayne, P.W., and Styler, M., 2018. Soil liquefaction screening using CPT yield stress profiles. In *Proc., Geotechnical Earthquake Engineering and Soil Dynamics V: Liquefaction Triggering, Consequences, and Mitigation*, edited by S. J. Brandenburg and M. T. Manzari, 12. Reston, VA: ASCE.

Neely, W.J., and Leroy, D.A., 1991. Densification of sand using a variable frequency vibratory probe. In *Proc., ASTM Symp. on Design, Construction and Testing of Deep Foundation Improvement: Stone Columns and Related Techniques*, edited by R. C. Bachus, 320–332. West Conshohocken, PA: ASTM.

Nguyen, T.V., Shao, L., Gingery, J., and Robertson, P.K., 2014. Proposed modification to CPT-based liquefaction method for post-vibratory ground improvement. In *Proc., ASCE Geo-Congress 2014 Technical Papers: Geo-Characterization and Modeling for Sustainability*, edited by M. Abu-Farsakh, X. Yu, and L. R. Hoyos, 1120–1132, Reston, VA: ASCE.

Robertson, P.K., 2016. Estimating K_0 in sandy soils using the CPT. In *Proc., 5th Int. Conf. on Geotechnical and Geophysical Site Characterization*. Gold Coast, QLD: Australian Geomechanics Society (AGS).

Robertson, P.K., and Campanella, R.G., 1983. Interpretation of cone penetrometer tests, Part I sand and Part II clay. *Can. Geotech. J.* 20 (4): 718–733. https://doi.org/10.1139/t83-078.

Robertson, P.K., Campanella, R.G., Gillespie, D., and Greig, J., 1986. Use of piezometer cone data. In *Proc., In-Situ'86 Use of In-Situ Testing in Geotechnical Engineering*, 1263–1280. Reston, VA: ASCE.

Schmertmann, J.H., 1985. Measure and use of the in-situ lateral stress. In *Proc., The practice of foundation engineering, a volume honoring Jorj O. Osterberg*, edited by R. J. Krizek, C. H. Dowding, and F. Somogyi, 189–213. Evanston, IL: Dept. of Civil Engineering.